The Structure and Properties of a Novel Nanocomposite Films from Chitosan and Layered Zirconium Phosphonate

Changhua Liu, Haixia Wu, Yajuan Yang, Lina Zhu, Yingli Teng

College of Chemistry and Chemical Engineering, Southwest University, 400715, Chongqing, China

Received 14 January 2010; accepted 21 August 2010
DOI 10.1002/app.33253
Published online 8 November 2010 in Wiley Online Library (wileyonlinelibrary.com).

ABSTRACT: A new type of layered zirconium phosphonate (zirconium glycine-*N*, *N*-dimethylphosphonate, abbreviated as ZGDMP), with functional group of -COOH, has been successfully prepared and characterized by Fourier transform infrared (FTIR) spectroscopy, X-ray diffraction (XRD), scanning electron microscopy (SEM) and transmission electron microscopy (TEM). To confirm the effect of the functional group -COOH on the structure and properties of composites, a series of chitosan/zirconium phosphonate modified by *n*-butylamine (BA-ZGDMP) nanocomposite films were prepared by casting process. FTIR spectra suggested that strong interactions existed between BA-ZGDMP and chitosan matrix. Compared to neat CS film, tensile strength (σ_b) and elongation at break (ε_b) of the nanocomposite film improved by 35.1% and 15.6%, respectively, with loading ratio of just 1.0 wt %. In addition, the BA-ZGDMP also improved the water resistance of the nanocomposites. © 2010 Wiley Periodicals, Inc. J Appl Polym Sci 120: 1106–1113, 2011

Key words: chitosan; zirconium glycine-*N*, *N*-dimethylphosphonate; nanocomposite films; structure; properties

INTRODUCTION

Polymer nanocomposites based on intercalated and exfoliated layered particles, as a new generation of advanced composites, have been extensively studied due to their excellent physical and mechanical properties, enhanced gas barrier properties, as well as superior flame retardancy.[1–7] The vast majority of such nanocomposites are based on graphite, Metal chalcogenides, Carbon oxides, Metal phosphates, Clays and layered silicates and Layered double hydroxides.[1] Among these, α-Zirconium phosphate (α-$Zr(HPO_4)_2$, hereafter α-ZrP), a synthetic layered structure material, has exhibited superiority over layered silicate as nanofiller such as ease of dimensional control, much higher purity and ion exchange capacity, easier process of intercalation/exfoliation, and more controllable surface functionality.[8] Furthermore, the particle size and aspect ratio can be manipulated by varying the reaction conditions.[9,10] It was firstly synthesized by Clearfield[11] and since then a wide range of studies have shown that tailor-made α-ZrP can be prepared: not only shape and size can be controlled by altering the reaction conditions, but its surface can be also easily modified to make it compatible to different polymers. There are several reports using α-zirconium phosphate as nanofiller that effectively improve the properties of polymers.[12–16] Yang et al.[13] improved the physical and mechanical properties of polyvinyl alcohol nancomposites with only a small amount of α-ZrP incorporated. Liu et al.[14] investigated the effects of aspect ratio, surface area and dispersion of α-ZrP on the properties of polyvinyl alcohol nancomposites. Wu et al.[15] successfully incorporated well-dispersed α-ZrP into chitosan matrix and significantly improved the mechanical properties of chitosan-based nanocomposite films.

It is well known that the interface interaction between the fillers and matrix severely affects the properties of the composite, especially mechanical properties. Surface treatment of fillers is the technique most often used to modify interactions in particulate-filled polymers.[17–20] A α-zirconium phosphate derivative, zirconium glycine-*N*, *N*-dimethylphosphonate (abbreviated as ZGDMP), with functional group of -COOH, has been successfully prepared. After *n*-butylamine modification, the functional group -COOH of ZGDMP was transformed to $-COO^-$ (abbreviated as BA-ZGDMP). Compared with the modified ways reported in the literature, our designed nanofillers (ZGDMP) possess organic groups (-COOH) linked with the inorganic layers through covalent bond, which can improve the first interface interaction between modified organic reagent and nanofillers. Moreover, it can be anticipated that the second interface interaction can be further enhanced by hydrogen bond or van der waals force between polymer matrix and nanofillers.

Correspondence to: C. Liu (chliu@swu.edu.cn).

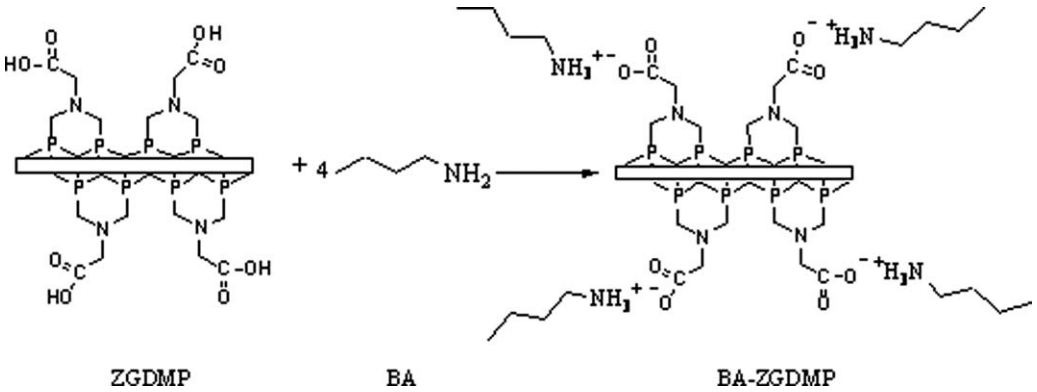

Scheme 1 The modified separate reaction scheme of ZGDMP.

On the basis of forenamed hypothesis, to confirm the feasibility of this design, chitosan was chosen as polymer matrix because the amino group (-NH_2) of chitosan can be protonated to -NH_3^+ and readily form electrostatic interactions with anionic groups in acidic media. It is therefore anticipated that modified fillers (BA-ZGDMP) with -COO^- would form stronger electrostatic interactions with -NH_3^+ of chitosan in acidic media in comparison with our previous work on α-ZrP reinforced chtiosan system,[15] which can result in stronger interfacial interaction between BA-ZGDMP and CS matrix and endow the composites with better properties.

In this work, a series of chitosan/zirconium phosphonate (CS/BA-ZGDMP) nanocomposite films were firstly prepared by casting process. Their structures were characterized by Fourier Transform Infrared (FTIR), Scanning electron microscopy (SEM), and X-ray diffraction (XRD) techniques. Thermal stability was confirmed by TG analysis. The moisture uptake of the nanocomposites was also evaluated.

EXPERIMENTAL

Materials

Chitosan (CS) was purchased from Nantong Xincheng Biological Industrial Limited Company (Nantong, China) with a weight-average molecular weight (M_w) of 300 000 g/mol and 90% degree of deacetylation. Acetic acid (36%) was obtained from Maoye Chemical Company (Chongqing, China). Zirconium oxychloride octahydrate ($ZrOCl_2{\cdot}8H_2O$) (99%) was purchased from Tianjin Kermel Chemical Reagent Development Center (Tianjin, China). *N, N*-bis(phosphonomethyl)-glycine ($(H_2O_3PCH_2)_2NCH_2$-COOH, hereafter DMPG) was synthesized according to literature.[21] *n*-Butylamine (99%) was supplied by Chengdu Kelong Chemical Reagent Company (Chengdu, China). Hydrofluoric acid (40%) was purchased from Chongqing Beibei Chemical Reagent Factory (Chongqing, China).

Synthesis and modification of Zgdmp

ZGDMP was prepared according to the following procedure. A solution of DMPG (9.12 g, 0.04 mol) in 50 mL water was added to $ZrOCl_2{\cdot}8H_2O$ (0.02 mol, 6.45 g) in 50 mL water with vigorous stirring and refluxed at 110°C for 24 h. The precipitate was filtered and washed using de-ionized water to pH = 5 ~ 6 and dried at 60°C under vacuum.

The prepared ZGDMP was intercalated by *n*-butylamine in an aqueous dispersion system (1.5 g/L) with a molar ratio of 0.8 (*n*-butylamine to ZGDMP). This was followed by a 0.5 h ultrasonic treatment and then stirred for five days at room temperature. The modified separate reaction scheme is shown in Scheme 1.

Film preparation

Chitosan solution was prepared by dissolving chitosan (CS) in a 2% (v/v) aqueous acetic acid solution at a concentration of 2 wt %, and followed by centrifuging to remove the insoluble materials. The modified ZGDMP (BA-ZGDMP) was then added to the chitosan solution, followed by stirring at 60°C for 5 h. After degassing under vacuum, the composite was cast onto glass plates and then dried at 55°C for 12 h to obtain dry film. The dried film was peeled off and kept in desiccators at 43% relative humidity at room temperature. By adjusting BA-ZGDMP loading levels to 0.5, 1.0, 1.5, and 2.0 wt %, respectively, a series of nanocomposite films with a thickness of around 0.1 mm were prepared and coded as CS/BA-ZGDMP-n (where n represented the BA-ZGDMP loading level). The codes of samples are listed in Table I.

FTIR spectroscopy

FTIR spectra of the nanocomposites were recorded on a Nicolet (Madison, WI) 170SX Fourier transform infrared spectrometer in the wavelength range of

TABLE I
Sample Codes and T_{max} of CS/BA-ZGDMP Nanocomposite Films Measured from the TGA

Code	CS/BA-ZGDMP-0	CS/BA-ZGDMP-1	CS/BA-ZGDMP-2	CS/BA-ZGDMP-3	CS/BA-ZGDMP-4
BA-ZGDMP (wt %)	0	0.5	1.0	1.5	2.0
T_{max} (°C)	269.87	272.39	271.13	277.43	271.13

4000–500 cm^{-1}, in the attenuated total reflection mode.

X-ray diffractometry

XRD patterns of the samples were carried out with a XRD-3D, PuXi (Beijing, China) X-ray diffractometer under the following conditions: Nickel filtered Cu$K\alpha$ radiation ($\lambda = 0.15406$ nm) at a voltage of 36 kV and current of 20 mA. The scanning rate was 4°/min.

Scanning electron microscopy

The cross sections of CS/BA-ZGDMP-n nanocomposite films were mounted on SEM stubs with double sided adhesive carbon tape, and then coated with gold in a 13.3 Pa vacuum degree. A scanning electron microscope (*S*-4800, HITACHI, Japan) was used to observe the morphologies of cross sections of the films at an accelerating voltage of 5 kV. The morphologies of the pristine ZGDMP and modified ZGDMP (BA-ZGDMP) powders were observed at an accelerating voltage of 20 kV.

Transmission electron microscopy

The transmission electron microscopy (TEM) micrograph was obtained on an H-7500 transmission electron microscope (HITACHI Co., Japan) at an accelerating voltage of 75 kV. Ultrathin sections were microtomed at room temperature.

Thermogravimetric analysis

Thermogravimetric (TG) and differential thermogravimetric (DTG) analyses of the CS/BA-ZGDMP-n nanocomposite films were carried out on a TA-STDQ600 (TA Instruments Inc., New Castle, USA). The thermograms were acquired between 20 and 500°C at a heating rate of 10°C/min. Nitrogen was used as the purge gas at a flow rate of 20 mL/min. An empty Al_2O_3 pan was used as a reference.

Mechanical properties

The tensile strength and elongation at break of the films were determined using a Micro-electronics Universal Testing Instrument Model Sans 6500 (Shenzhen Sans Testing Machine Co. Ltd., Shenzhen, China) according to the Chinese standard method (GB 13022-91). The films were cut into 10 mm wide and 100 mm long strips and mounted between cardboard grips (150 × 300 mm^2) using adhesive so that the final area exposed was 10 × 50 mm^2. Before testing, the samples were kept at 43% *RH* at room temperature for more than one week to ensure equilibration of the moisture uptake in the films. The cross-head speed was 10 mm/min. All measurements were performed on three specimens and averaged.

Moisture uptake test

The moisture uptake of the nanocomposite films was determined on samples that were thin rectangular strips with dimensions of 50 mm ×10 mm ×0.1 mm. The samples were dried overnight at 80°C, weighed, and then conditioned for two weeks at 92%RH (Na_2CO_3 saturated solution) to ensure equilibrium of the moisture before reweighing. The moisture uptake (Mu) of the samples was calculated as follows:

$$\mathrm{Mu} = (W_1 - W_0)/W_0 \times 100\%$$

where W_0 and W_1 were the weights of the sample before exposure to 92% RH and after equilibrium, respectively. An average value of three replicates for each sample was taken.

RESULTS AND DISCUSSION

Fourier transform infrared spectroscopy

The FTIR spectra of pristine ZGDMP and modified ZGDMP (BA-ZGDMP) powders are shown in Figure 1(a). In the pristine ZGDMP (curve A), a characteristic strong peak at 3445 cm^{-1} was attributed to O—H stretching. The peaks at 1737 and 1425 cm^{-1} were assigned to C=O stretching and O—H bending of -COOH group, respectively.[22] The bands occurred at 1640 and 1029 cm^{-1} associated with the δ(O—H) bending of water and P—O stretching, respectively. After intercalation of *n*-butylamine into ZGDMP, the bands occurred at 1737 and 1425 cm^{-1}, which can be attributed to the -COOH vibrations, disappeared and the bands attributed to the $-COO^-$ appeared at 1396 and 1555 cm^{-1}. Bands corresponding to $-NH_3^+$

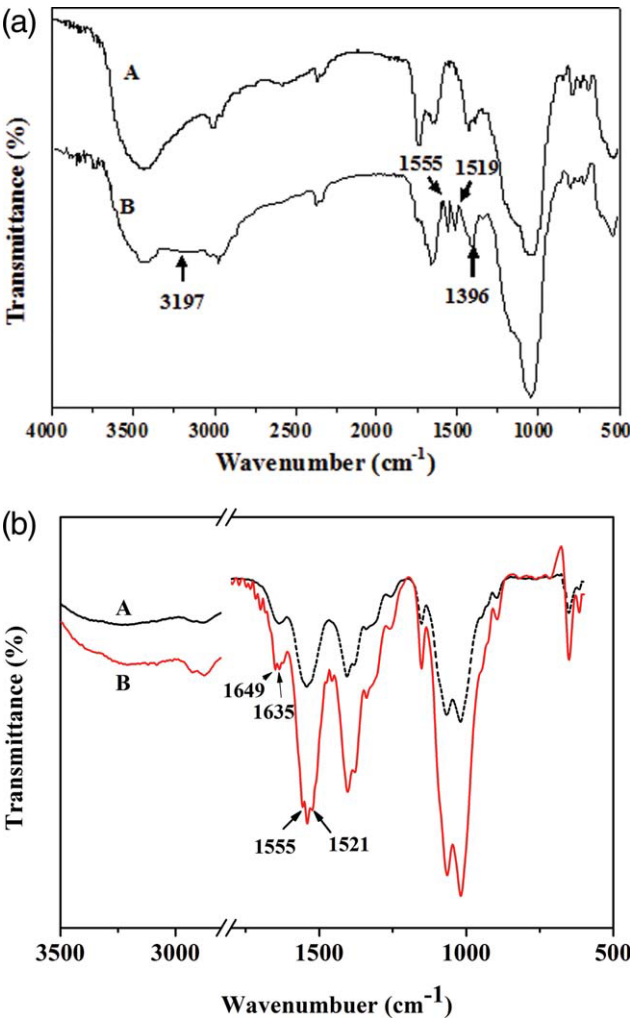

Figure 1 (a). FTIR spectra of pristine ZGDMP (A) and BA-ZGDMP (B). (b). FTIR spectra of neat chitosan film (A) and CS/BA-ZGDMP-2 nanocomposite film (B). [Color figure can be viewed in the online issue, which is available at wileyonlinelibrary.com.]

were also detected and occurred at 3197 and 1519 cm^{-1}. These results revealed that *n*-butylamine was intercalated into ZGDMP in such a way that the protons of the interlayer -COOH groups were replaced by the terminal $-NH_3^+$ of the protonated *n*-butylamine.

Figure 1(b) shows FT-IR spectra of the neat chitosan film (curve A) and CS/BA-ZGDMP-2 nanocomposite film (curve B). The IR spectrum of neat chitosan film was very similar to that found in the previous report.[23] In the spectrum of neat chitosan film (curve A), a characteristic strong peak at 3231 cm^{-1} was attributed to overlapping stretching vibrations of $-NH_2$ and -OH groups.[24] A small peak occurred at 1636 cm^{-1} was attributed to the presence of acetyl unit with —C=O stretching because of 90% deacetylation.[25] The strong peak at 1543 cm^{-1} was attributed to N—H bending. The peaks near 2881 cm^{-1} were typical C—H stretching vibrations. The absorption band at 1152 cm^{-1} was assigned to the antisymmetric stretching of C—O—C bridge. The peaks at 1066 and 1019 cm^{-1} were attributed to the skeletal vibrations involving the C—O stretching.[26] The IR spectrum for CS/BA-ZGDMP-2 showed a complex spectrum from CS and BA-ZGDMP. Although these characteristic absorption bands for CS/BA-ZGDMP-2 showed no significant wavenubmer changes in comparison with the BA-ZGDMP and CS IR spectrum, the characteristic absorption peak of chitosan at 3231 cm^{-1} shifted to 3080 cm^{-1} and the intensity increased. This may be attributed that the interaction between the negatively charged $-COO^-$ of BA-ZGDMP and the positively charged $-NH_3^+$ of chitosan matrix in CS/BA-ZGDMP-2 was the same as that in neat chtiosan film since the chitosan film prepared using acetic acid as a dissolving vehicle was chitosonium acetate film.[23] These results indicated that the hydrogen-bond interactions and electrostatic interactions generated in CS/BA-ZGDMP complex films.

X-ray diffractometry

XRD patterns of pristine ZGDMP and modified ZGDMP (BA-ZGDMP) powders are shown in Figure 2(a). The XRD pattern suggested that ZGDMP was semicrystalline probably resulted from the absence of HF. This was similar to that found by Zeng et al.[27] Because of the effect of dimethylphosphonate groups with one organic residue, $(-CH_2)_2NCH_2COOH$, in the interlayer region, the interlayer *d*-spacing of ZGDMP corresponding to diffraction peak $2\theta = 6.54°$ was about 1.35 nm, which was much larger than that of α-ZrP ($d = 0.76$ nm). When ZGDMP was intercalated by *n*-butylamine, the diffraction peaks $2\theta = 6.54°$ ($d = 1.35$ nm) of ZGDMP shifted to the lower Bragg's angles $2\theta = 5.01°$ corresponding to the interlayer distance of 1.76 nm, indicating that *n*-butylamine was successfully intercalated into the galleries of ZGDMP.

The XRD patterns of CS/BA-ZGDMP-n nanocomposite films are shown in Figure 2(b). The neat chitosan film (CS/BA-ZGDMP-0) showed three main diffraction peaks around $2\theta = 11.4°$, 18.3° 22.9°, as well as two broad peaks around $2\theta = 8.3°$, 16.1° with low intensity in the XRD patterns, which agreed with the previous report.[28] It could be clearly observed that the additive BA-ZGDMP had no great influence on the crystal type of CS-based nanocomposite films. The CS-based nanocomposite films showed XRD patterns very similar to that of the neat chitosan film. It was difficult to find the characteristic diffraction peaks of BA-ZGDMP in the composites, probably due to low loading and poor crystallinity of BA-ZGDMP, but also indicated that the BA-

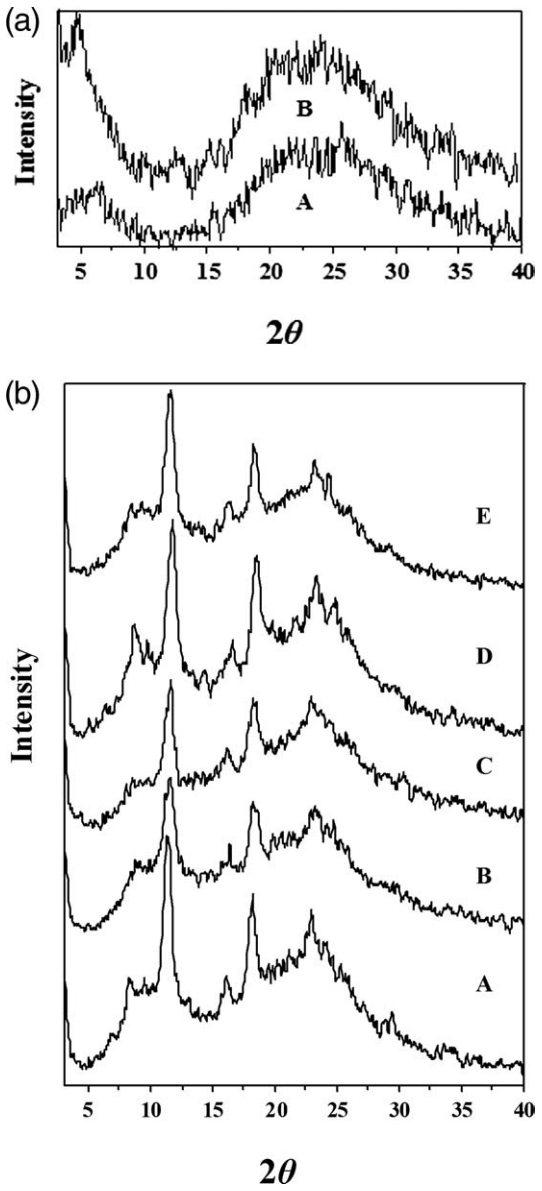

Figure 2 (a). XRD patterns of pristine ZGDMP (A) and BA-ZGDMP (B). (b). XRD patterns of CS/BA-ZGDMP-0 (A), CS/BA-ZGDMP-1 (B) CS/BA-ZGDMP-2 (C), CS/BA-ZGDMP-3 (D), and CS/BA-ZGDMP-4 (E).

ZGDMP particles were well dispersed in the nanocomposites.[29]

Scanning electron microscopy

SEM micrographs of pristine ZGDMP, modified ZGDMP (BA-ZGDMP) powders, and the fracture surfaces of the films after tensile testing are shown in Figure 3. SEM images of ZGDMP (A) and BA-ZGDMP (B) showed significant differences in morphology. It was clearly observed that ZGDMP (A) exhibited a layered structure and irregular thin sheets with particle sizes varying approximately between 5 and 10 μm. ZGDMP also appeared semi-crystalline, which was proven by XRD pattern [Fig. 2(a), curve A]. The BA-ZGDMP appeared to be an aggregation of much smaller particles, which was probably ascribed to the fact that BA-ZGDMP had the larger surface energy and aggregated easily. The cross section of the neat CS film [Fig. 3(C)] was smooth, whereas the CS/BA-ZGDMP-2 composite films [Fig. 3(D)] became rough due to the incorporation of BA-ZGDMP. This probably resulted from the addition of BA-ZGDMP acting as the physical crosslinking agent the through the formation of strong electrostatic interactions between the negative $-COO^-$ groups of BA-ZGDMP and positive $-NH_3^+$ groups of chitosan matrix in acidic media, which resulted in some gel points on the cross sections of CS/BA-ZGDMP-2 films, whereas no obvious of aggregations of BA-ZGDMP were observed in SEM photographs. Because of the small size of BA-ZGDMP and homogeneous dispersion in CS matrix, the BA-ZGDMP might be wrapped tightly by the CS and could not be exposed. The strong adhesions between BA-ZGDMP and CS also prohibited the BA-ZGDMP from being exposed. As a result, no BA-ZGDMP was identified individually from the matrix in the SEM photographs of CS/BA-ZGDMP-2 film.

Transmission electron microscopy

More direct evidence for the formation of a nanocomposite is provided by TEM. TEM image of CS/BA-ZGDMP-2 is shown in Figure 4. The dark sheets were the BA-ZGDMP particles well-dispersed in the matrix of chitosan. The TEM picture of CS/BA-ZGDMP-2 shows the presence of exfoliated BA-ZGDMP particles having the largest dimension in the range 30–120 nm and thickness of 15–40 nm with aspect ratio of 2–3. In agreement with the exfoliation of the filler, it was difficult to find the characteristic diffraction peaks of BA-ZGDMP in the composites. The results corresponded well with the XRD results.

Thermogravimetric analysis

The thermal stability of the neat CS and their nanocomposites films was studied by thermogravimetric analysis (TGA) and differential thermogravimetry (DTG), presented in Figure 5(a,b), respectively. As can be seen, all samples showed the weight loss in two well-distinguished steps, which were more obvious in DTG curves. The first step recorded in the temperature range 30–150°C, corresponding to a mass loss of 8–15 wt %, was associated with the loss of adsorbed and bound water and the residue of acetic acid. The second step of weight loss in 200–350°C, which was the main decomposition step

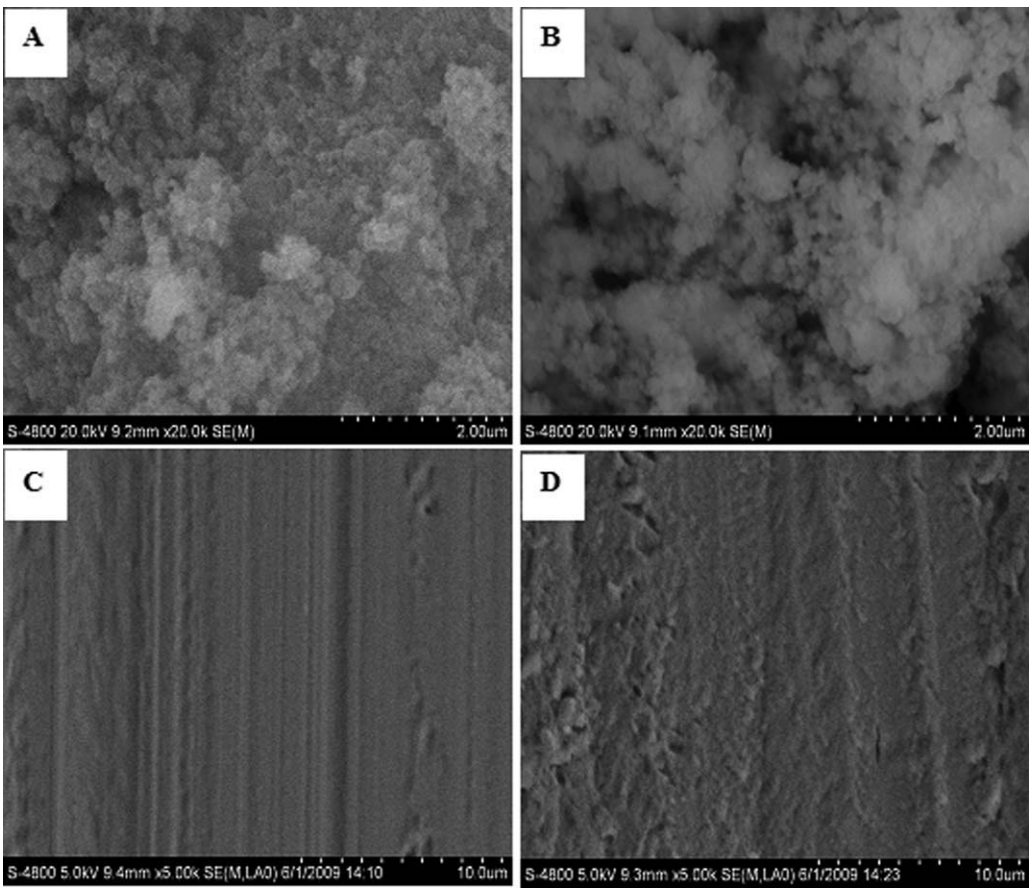

Figure 3 SEM micrographs of pristine ZGDMP (A), BA-ZGDMP (B) powders and fracture surface for the films: CS/BA-ZGDMP-0 (C), CS/BA-ZGDMP-2 (D).

(mass loss 40–50 wt %), corresponded to the degradation and deacetylation of chitosan.[30] T_{max} is the temperature corresponding to the maximum rate of degradation, which can be obtained from the DTG curve [Fig. 5(b)] and assess a material's thermal stability. T_{max} for all of the samples is summarized and listed in Table I. It was clearly observed that T_{max} of the nanocomposite films displayed no remarkable change within experimental error. The result indicated that the thermal stability of chitosan composite was not be affected by BA-ZGDMP loading.

Mechanical properties

The mechanical properties of nanocomposite films are measured and the results are presented in Figure 6. As can be seen, both the tensile strength (σ_b) and the elongation at break (ε_b) increased significantly with increasing amount of BA-ZGDMP to 1.0 wt %, followed by a decrease with further increase to 2.0 wt %. When 1.0 wt % BA-ZGDMP was added, σ_b and ε_b of the nanocomposite film reached the maximum values of 63.73 MPa and 54.2%, respectively, approximately increased by 35.1% and 15.6% compared to those of neat chitosan film. The substantial

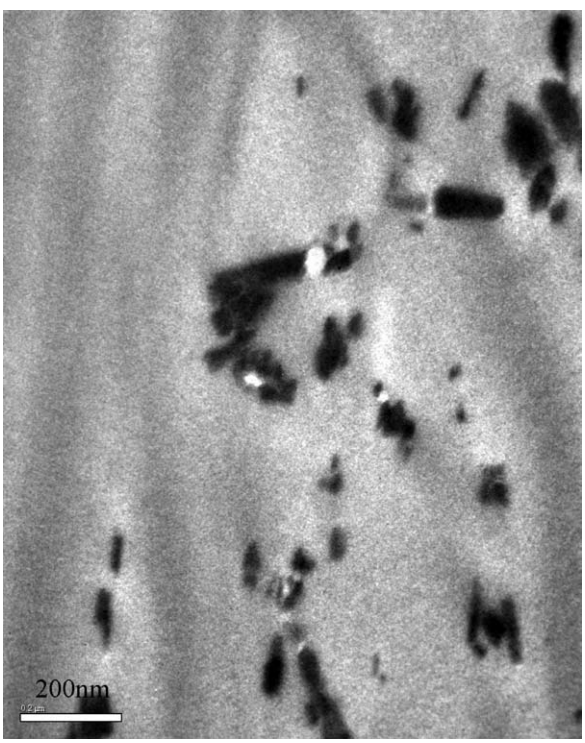

Figure 4 TEM micrograph of CS/BA-ZGDMP-2.

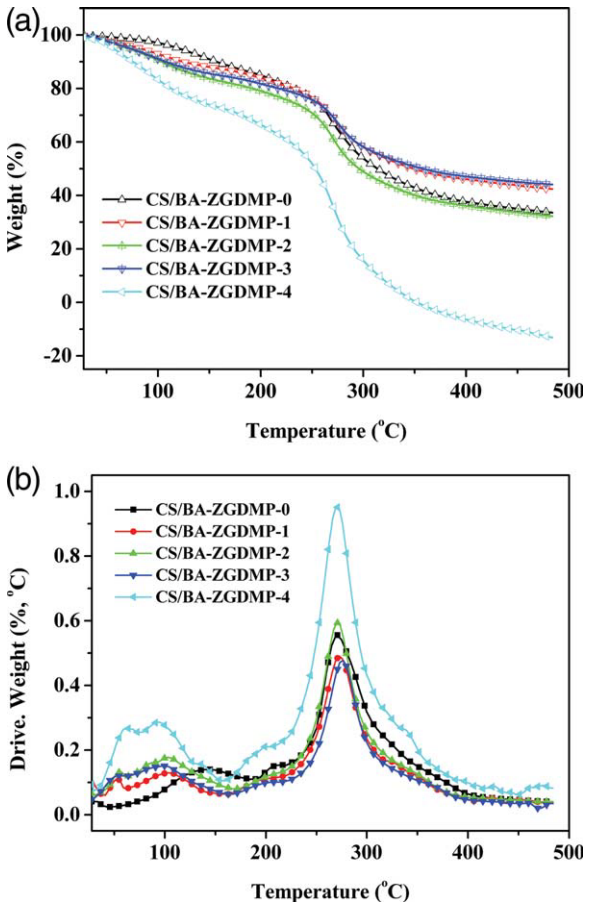

Figure 5 (a). TGA curves of CS/BA-ZGDMP-n nanocomposite films. (b). DTG curves of CS/BA-ZGDMP-n nanocomposite films. [Color figure can be viewed in the online issue, which is available at wileyonlinelibrary.com.]

improvement of σ_b and ε_b with the addition of a small amount of BA-ZGDMP was ascribed to the formation of stronger electrostatic interactions between chitosan and BA-ZGDMP. The decrease in mechanical properties with increasing BA-ZGDMP loading up to 2.0 wt % resulted from the aggregation of BA-ZGDMP particles with high surface energy when the BA-ZGDMP loading was high enough. In our previous work, α-ZrP-reinforced chtiosan system,[15] σ_b and ε_b achieved the maximum value 61.6 MPa and 58.1%, respectively, with incorporated 2 wt % of α-ZrP. We can find that the maximum σ_b of CS/BA-ZGDMP system was slightly higher than that of the CS/ZrP system, whereas the maximum ε_b of CS/BA-ZGDMP system was slightly lower than that of the CS/ZrP system. Furthermore, the BA-ZGDMP loading was only 1 wt % BA-ZGDMP at the maximum values of the mechanical properties, which was the half loading level in the CS/ZrP system. The results demonstrated that introduction of organic groups can effectively enhance the interfacial interactions between the fillers and matrix and improve the properties of composite.

Moisture uptake of the films

Figure 7 illustrates the influences of the BA-ZGDMP loading on the moisture uptake (Mu) of the films under 92% *RH* for 7 days. It was found that the Mu value of neat chitosan film in this condition was 76%. The Mu value of naocomposites significantly decreased as the BA-ZGDMP content increased and reached the minimum of 50% when the BA-ZGDMP content was 1.0 wt %. This suggested that the addition of BA-ZGDMP effectively decreased the moisture uptake of the CS-based composites, which resulted from the strong interactions formed between molecules of chitosan matrix and BA-ZGDMP particles, which obstructed and weakened the diffusion of water molecules in the material.

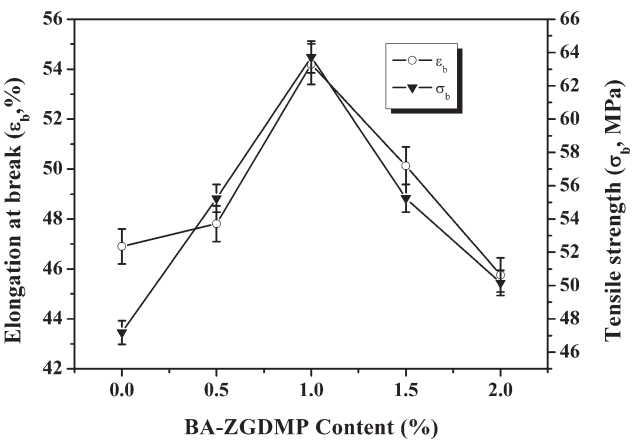

Figure 6 The mechanical properties of CS/BA-ZGDMP nanocomposite films with different BA-ZGDMP contents.

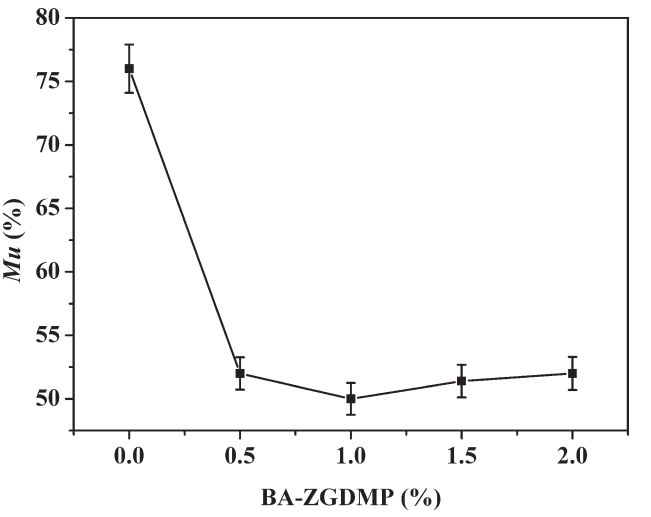

Figure 7 Moisture uptake (Mu) at equilibrium of the CS/BA-ZGDMP-n nanocomposite films.

CONCLUSIONS

In this study, a novel CS/BA-ZGDMP nanocomposite film has been successfully prepared and characterized, in which BA-ZGDMP was used as nanofiller. FT-IR spectra revealed that there existed strong interactions including electrostatic interactions and hydrogen-bond interactions between CS and BA-ZGDMP molecules. XRD, SEM, and TEM results showed that BA-ZGDMP dispersed uniformly in the chitosan matrix. The TEM picture of CS/BA-ZGDMP-2 shows the presence of exfoliated BA-ZGDMP particles with aspect ratio of 2–3. Both the tensile strength and elongation at break of the films were remarkably enhanced when a small amount of BA-ZGDMP was incorporated. The presence of BA-ZGDMP also decreased the moisture uptake of the nanocomposite films. It can be concluded that introduction of organic groups can enhance the interfacial interactions between the fillers and matrix of the composites.

References

1. Alexandre, M.; Dubois, P. Mater Sci Eng 2000, 28, 1.
2. Giannelis, E. P. Adv Mater 1996, 8, 29.
3. Ray, S. S.; Okamoto, M. Prog Polym Sci 2003, 28, 1539.
4. Lan, T.; Kaviratna, P. D.; Pinnavaia, T. J Chem Mater 1995, 7, 2144.
5. Shi, H.; Lan, T.; Pinnavaia, T. J Chem Mater 1996, 8, 1584.
6. Yano, K.; Usuki, A.; Okada, A.; Kurauchi, T.; Kamigaito, O. J Polym Sci Pol Chem 1993, 31, 2493.
7. Zhu, J.; Start, P.; Mauritz, K. A.; Wilkie, C. A. Polym Degrad Stabil 2002, 77, 253.
8. Sun, L.; Boo, W. J.; Sun, D.; Clearfield, A.; Sue, H.-J. Chem Mater 2007, 19, 1749.
9. Sun, L.; Boo, W. J.; Browning, R. L.; Sue, H.-J.; Clearfield, A. Chem Mater 2005, 17, 5606.
10. Boo, W.-J.; Sun, L.; Warren, G. L.; Moghbelli, E.; Pham, H.; Clearfield, A.; Sue, H.-J. Polymer 2007, 48, 1075.
11. Clearfield, A.; Stynes, J. A. J Inorg Nucl Chem 1964, 26, 117.
12. Wu, H.; Liu, C.; Chen, J.; Chang, P. R.; Chen, Y.; Anderson, D. P. Carbohyd Polym 2009, 77, 358.
13. Yang, Y.; Liu, C.; Wu, H. Polym Test 2009, 28, 371.
14. Liu, C.; Yang, Y. Polym Test 2009, 28, 801.
15. Wu, H.; Liu, C.; Chen, J.; Yang, Y.; Chen, Y. Polym Int 2010, 59, 923.
16. Yang, Y.; Liu, C.; Chang, P. R.; Chen, Y.; Anderson, D. P.; Stumborg, M. J Appl Polym Sci 2010, 115, 1089.
17. Demjen, Z.; Pukanszky, B.; Nagy, J. Compos A 1998, 29, 323.
18. Han, C. D.; Weghe, T. V. D.; Shete, P.; Haw, J. R. Polym Eng Sci 1981, 21, 196.
19. Nakatsuka, T.; Kawasaki, H.; Itadani, K.; Yamashita, S. J Appl Polym Sci 1979, 24, 1985.
20. Ishida, H.; Miller, J. D. Macromolecules 1984, 17, 1659.
21. Moedritzer, K.; Irani, R. R. J Org Chem 1966, 31, 1603.
22. Raghu, A. V.; Gadaginamath, G. S.; Jeong, H. M.; Mathew, N. T.; Halligudi, S. B. J Appl Polym Sci 2009, 113, 2747.
23. Nunthanid, J.; Puttipipatkhachorn, S.; Yamamoto, K.; Peck, G. E. Drug Dev Ind Pharm 2001, 27, 143.
24. Xu, Y. X.; Kim, K. M.; Hanna, M. A.; Nag, D. Ind Crop Prod 2005, 21, 185.
25. Pearson, F. G.; Marchessault, R. H.; Liang, C. Y. J Polym Sci 1960, 43, 101.
26. Kweon, H. Y.; Um, I. C.; Park, Y. H. Polymer 2001, 42, 6651.
27. Zeng, R.; Fu, X.; Sui, Y.; Yang, X.; Sun, M.; Chen, J. J Organomet Chem 2008, 693, 2666.
28. Tang, C.; Xiang, L.; Su, J.; Wang, K; Yang, C.; Zhang, Q.; Fu, Q. J Phys Chem B 2008, 112, 3876.
29. Boo, W. J; Sun, L. Y.; Liu, J.; Moghbelli, E.; Cleafield, A; Sue, H. J.; Pham, H.; Verghese, N. J Polym Sci Part B 2007, 45, 1459.
30. Qu, X.; Wirsen, A.; Albertsson, A. C. Polymer 2000, 41, 4841.